Intramolecular Interactions That Induces Helical Rearrangement upon Rhodopsin Activation: Light-Induced Structural Changes in Metarhodopsin II_a Probed by Cysteine S-H Stretching Vibrations[*]

Yoichi Yamazaki[‡§], Tomoko Nagata[‡], Akihisa Terakita[‡¶], Hideki Kandori[‡||], Yoshinori Shichida[‡] and Yasushi Imamoto[‡1]

From the [‡]Department of Biophysics, Graduate School of Science, Kyoto University, Kyoto 606-8502, Japan, the [§]Graduate School of Materials Science, Nara Institute of Science and Technology, Nara, 630-0192, Japan, the [¶]Department of Biology and Geosciences, Graduate School of Science, Osaka City University, Osaka 558-8585, Japan, and the [||]Department of Frontier Materials, Graduate School of Engineering, Nagoya Institute of Technology, Nagoya 466-8555, Japan

[*]**Running title:** Intramolecular interaction in metarhodopsin II_a

[1]To whom correspondence should be addressed: Yasushi Imamoto, Department of Biophysics, Graduate School of Science, Kyoto University, Kyoto 606-8502, Japan, Tel.: +81-75-753-4243; Fax: +81-75-753-4210; E-mail: imamoto@rh.biophys.kyoto-u.ac.jp.

Key words: Fourier transform infrared spectroscopy, G protein coupled receptor, phototransduction, protein conformation, rhodopsin, vision

---

Background: Identification of the intramolecular interactions in metarhodopsin II_a is essential for understanding the activation mechanism of rhodopsin.
Results: Environmental changes around the chromophore, Ala164, His211 and Phe261 were observed by probing with cysteine S-H vibrations.
Conclusion: The interactions involving these residues are altered before the helical rearrangements.
Significance: The intramolecular interactions by which rhodopsin adopts the transducin-activating conformation is shown.

ABSTRACT

Rhodopsin undergoes rearrangements of its transmembrane helices after photon absorption to transfer a light signal to the G protein transducin. To investigate the mechanism by which rhodopsin adopts the transducin-activating conformation, the local environmental changes in the transmembrane region were probed using the cysteine S-H group, whose stretching frequency is well isolated from the other protein vibrational modes. The S-H stretching modes of cysteine residues introduced into Helix III, which contains several key residues for the helical movements, and of native cysteine residues were measured by Fourier transform infrared spectroscopy. This method was applied to metarhodopsin II_a, a precursor of the transducin-activating state in which the intramolecular interactions are likely to produce a state ready for helical movements. No environmental change was observed near the ionic lock between Arg135 in Helix III and Glu247 in Helix VI that maintains the inactive conformation. Rather, the cysteine residues that showed environmental changes were located around the chromophore, Ala164, His211, and Phe261. These findings imply that the hydrogen bond between Helix III and Helix V involving Glu122 and His211 and the hydrophobic packing between Helix III and Helix VI involving Gly121, Leu125, Phe261, and Trp265 are altered before the helical rearrangement leading towards the active conformation.

G-protein-coupled receptors (GPCRs)[2] are activated in response to various kinds of stimuli and in turn activate cognate G-proteins. GPCRs have common structural motifs consisting of seven transmembrane helices (1-3). Ligands bind to the extracellular surface of a GPCR and activate it. The activation occurs via rearrangements of transmembrane helices (4-6), which are likely to be common among GPCRs (7). Thus the ligand-induced changes in the intramolecular interactions that induce helical rearrangement should be clarified to understand the mechanisms of activation of GPCRs.

Many GPCRs have been identified, but rhodopsin, which absorbs photons in rod photoreceptor cells, is biochemically, structurally, and physicochemically the best characterized. Rhodopsin consists of a protein moiety called opsin and an 11-*cis*-retinal chromophore which absorbs a photon. The chromophore is covalently bound to Lys residue in Helix VII of opsin through a Schiff base linkage. Photo-isomerization of the chromophore initiates conformational changes of opsin leading to the formation of several intermediate states. Among these states, metarhodopsin II (Meta-II) is thought to activate the G protein transducin (Gt).

Meta-II has an absorption spectrum in the near-UV region, unlike the dark state or the other intermediates. This is mainly because the Schiff base linkage between opsin and chromophore is deprotonated in Meta-II. Meta-II is activated via the significant rearrangement of the transmembrane helices (4-6), as confirmed by the crystal structure of the complex of Meta-II and C-terminal peptide of Gt (8-10). Meta-II forms a pH- and temperature-dependent equilibrium with its precursor metarhodopsin I (Meta-I) (11-14). Recent extensive studies on metarhodopsins have demonstrated that Meta-II is the equilibrium mixture composed of several species (Scheme 1) (14-18). Meta-I is in pH-independent thermal equilibrium with Meta-II_a and Meta-II_b. Although both Meta-II_a and Meta-II_b have a deprotonated Schiff base, Meta-II_a displays only minor helical rearrangements. This mixture is in pH-dependent equilibrium with Meta-II_bH^+, which binds to and activates Gt.

The intramolecular interactions in rhodopsin are altered essentially by the proton movement from the protonated Schiff base to the conterion (Glu113). While the helical arrangement of Meta-II_a is comparable to those of the dark state or its precursors, the intramolecular interactions in Meta-II_a should be altered and these alterations should readily induce significant helical rearrangements. Thus, identification of the intramolecular interactions in Meta-II_a is essential for understanding the mechanism by which photoactivated rhodopsin adopts the active conformation (18)

In the present study, using Fourier transform infrared (FTIR) spectroscopy (19), we detected the structural changes in the transmembrane region by monitoring changes in the S-H stretching vibration of the cysteine residues present in native rhodopsin or of cysteine residues systematically introduced into the transmembrane region. There are some advantages of using cysteine as a probe: First, depending on the environment, the cysteine S-H stretching frequency is in the 2580-2525 cm^{-1} region, which is well-separated from vibrations of the other groups present in protein (20-23). Thus, changes of the environment of the cysteine can be probed without interference from other vibrational modes. Second, cysteine can be accommodated in the transmembrane region because of its relatively small and hydrophobic nature. Third, cysteine residues are introduced using a well-established point-mutation technique, which is simpler than the recently developed method using a non-natural amino acid *p*-azido-L-phenylalanine (azF) (24).

We have developed this method for mapping the amino acid residues which undergo environmental changes (cysteine scanning) and applied it to bathorhodopsin, whose high-resolution crystal structure is available (23). It was confirmed that cysteine residues introduced near the chromophore showed the clear shift in the S-H stretching mode in response to the local conformational change but those introduced into the part were completely silent. In the present study, Meta-II_a (15, 17, 18) was characterized by cysteine scanning. We targeted the cysteine residues introduced into Helix III because it contains several functionally and structurally important residues, such as Glu113, Glu122, and Glu134 (25-29), and the separation of Helix III from Helix VI is the key event for the activation of rhodopsin.

EXPERIMENTAL PROCERURES

Preparation of Rhodopsin and Its Cysteine Mutants- Wild-type and mutant bovine opsin genes were expressed in HEK 293S cell lines as previously reported (30, 31). cDNAs were fully sequenced before introduction into the expression vector, pUSRα. To reconstitute the pigments, membrane fragments containing expressed opsins were incubated with 11-*cis*-retinal for more than 3 h at 4°C. The pigments were extracted with 1% (w/v) dodecyl-β-D-maltoside (DM) in buffer P (50 mM HEPES, 140 mM NaCl, pH 6.5). The extracts were incubated with rho 1D4 antibody-agarose gel at room temperature overnight. After washing with buffer A (0.02% DM in buffer P), the pigments were eluted with buffer A containing the C-terminal octadecapeptide of rhodopsin (DEASTTVSKTETSQVAPA). The UV-visible spectra were recorded at this stage to estimate the

absorption maximum in the visible region and optical purity index with a Shimadzu MPS-2000 recording spectrophotometer.

Solubilized rhodopsins were supplemented with a 100-fold molar excess of PC (Type XI-E, Sigma P2772), and dialyzed against buffer P for 3-4 days at 4 °C. Rhodopsins in PC liposomes had absorbance in the range of 0.02 to 0.1. Liposomes were then collected by centrifugation, and re-suspended in 1 mM phosphate buffer (pH 5.7) supplemented with 5 mM NaCl. Sixty microliters of suspensions were placed on a BaF_2 window and dried under vacuum using an aspirator. The sample was sealed using another BaF_2 window and a spacer after ~1 μl of H_2O was put beside the sample.

Spectroscopy- FTIR spectra were recorded using a Bio-Rad FTS40K spectrometer. An Oxford DN-1704 cryostat connected to an Oxford ITC-4 temperature controller was used for maintaining the sample temperature at 280.0 ± 0.1 K. Irradiation light (>520 nm) was generated using a 1-kW tungsten halogen lamp (Rikagaku Seiki) and passed through a glass cutoff filter (O54, Toshiba). The Meta-II_a minus rhodopsin difference spectra (Meta-II_a/Rho spectra) were obtained by irradiation with >520-nm light at 280 K for 30 sec. For each measurement, 256 interferograms at 2 cm^{-1} resolution were recorded. Meta-II_a/Rho spectra were the averages of at least two measurements.

RESULTS

Effect of Mutation on the Absorption Maxima- Wild-type rhodopsin has 10 cysteine residues (Figure 1), among which Cys322 and Cys323 are palmitoylated, and Cys110 and Cys187 form a disulfide bond. Thus 6 out of 10 native cysteine residues have free S-H groups, and were replaced with serine (C140S, C167S, C185S, C222S, C264S, and C316S). We also prepared a double mutant C110A/C187A, because a previous FTIR study focusing on S-H groups suggested the possible cleavage of the disulfide bond formed by these residues (21). In addition, 15 cysteine-introduced mutants at positions 117, 118, and 122-134 were prepared to probe the environmental changes along Helix III. We first examined the effects of these replacements of the native cysteine residues and introductions of cysteine residues.

All of these mutants were reconstituted into pigments with 11-*cis*-retinal. In addition, difference FTIR spectra between these mutants and their barho intermediates are comparable to that of wild-type (23). These findings indicate that the overall structure of rhodopsin is little perturbed by these mutations. Absorption maxima (λ_{max}) of mutants and optical purity indexes (ratio of absorbance at 280 nm to absorbance at λ_{max}) of the samples are listed in Table 1. Whereas the absorption maxima of most mutants were similar to that of the wild-type (499 nm), mutations near the chromophore caused relatively large blue-shifts of the absorption maxima (A117C, T118C, and W126C). However, the difference FTIR spectra for Batho of these mutants agreed with those of wild-type except for the chromophore bands, indicating that the perturbation of these mutations is limited to the vicinity of the chromophore (23).

In some samples, optical purity index was >3, indicating that significant amount of opsin and/or other proteins are present in the sample. However, because the difference FTIR spectra before and after visible light irradiation were measured in the following experiments, the proteins which are not photoactive (e.g. opsin) should not contribute to the FTIR spectra.

Formation of Metarhodopsin II_a in Hydrated Phosphatidylcholine Liposomes- Meta-II_a is the intermediate state in which the chromophore Schiff base is deprotonated but the helical arrangement is similar to that of Meta-I (15, 17, 18, 32). In native rod outer segment (ROS) membrane, small amount of Meta-II_a is in equilibrium with Meta-I and Meta-II_b (Scheme 1). It has been reported that the amount of Meta-II_a in the equilibrium is increased in 1,2-dioleoyl-*sn*-glycero-3-phosphocholine (DOPC) membranes (18), and Meta-II_a in the equilibrium with significant amounts of Meta-I and Meta-IIb has been partially characterized by FTIR spectroscopy (18).

In the course of characterization of Meta-II by FTIR, we found that a difference FTIR spectrum whose characteristics agree with those of the Meta-II_a/Rho spectrum is obtained by irradiation of rhodopsin in hydrated film sample at 280 K, which was prepared by drying rhodopsin in PC liposomes suspended in the phosphate buffer at pH 5.7 followed by hydration by ~1 μl of H_2O (Figure 2). While Meta-II_a is favored at higher pH, this product is trapped at acidic pH, and is likely to be in the protonated form (Meta-II_aH^+) (see below). This putative Meta-II_aH^+/Rho spectrum is shown in Figure 2 in comparison with Meta-I/Rho and Meta-II_bH^+/Rho spectra. The Meta-I/Rho spectrum has an amide-I band at 1635 cm^{-1}, whereas the

Meta-II_bH^+/Rho spectrum has one at 1644 cm^{-1}. Since the Meta-II_aH^+/Rho spectrum has 1645 and 1635 cm^{-1} bands, it appears to be a mixture of Meta-I/Rho and Meta-II_bH^+/Rho spectra. In fact, synthetic spectra composed of 80% Meta-I/Rho and 20% Meta-II_bH^+/Rho spectra showed comparable intensities of the 1645 and 1635 cm^{-1} bands (Figure 3). However, the 949 cm^{-1} band typical of the Meta-I/Rho spectrum (33, 34) disappeared in the Meta-II_aH^+/Rho spectrum, indicating that the Meta-II_aH^+/Rho spectrum cannot be generated by a linear combination of Meta-I/Rho and Meta-II_bH^+/Rho spectra. These findings confirm that the Meta-II_aH^+/Rho spectrum obtained in the present condition is the difference FTIR spectrum between isolated Meta-II_aH^+ and rhodopsin.

It should be noted that the irradiation of native rhodopsin in the hydrated film of ROS in this condition generated a Meta-II_bH^+/Rho spectrum, unlike the spectrum obtained in PC liposomes (Figure 3). When the hydration level was reduced, a Meta-I-like photoproduct was produced in ROS membrane. Thus the stabilization of Meta-II_a in our experimental condition is likely to be caused by PC.

Characteristics of Meta-II_aH^+- The small amide-I band in the Meta-II_aH^+/Rho spectrum indicates that Meta-II_aH^+ undergoes small conformational change. The positive 1712 cm^{-1} band shows the protonation of Glu113 in Meta-II_aH^+/Rho (35). Asp83 and Glu122 show 1748/1769 cm^{-1} and 1745/1728 cm^{-1} bands, respectively, in the Meta-II_bH^+/Rho spectrum (36). Similar bands for Asp83 and Glu122 are also observed in the Meta-II_aH^+/Rho spectrum. However, the weak intensity of the positive 1748 cm^{-1} band would result from the reduced 1745/1728 cm^{-1} bands of Glu122. These characteristics of the Meta-II_aH^+/Rho spectrum are consistent with those of Meta-II_a (18).

To assess the protonation states of Glu residues in Meta-II_aH^+, the Meta-II_aH^+/Rho spectrum of the wild-type was compared with those of E122C and E134C (Figures 2d and 2e). The double difference spectra between the Meta-II_aH^+/Rho spectra of wild-type and E122C showed that the C=O stretching mode of Glu122 shifted from 1728 to 1745 cm^{-1} upon formation of Meta-II_aH^+. These frequencies are comparable to those of Meta-II_bH^+/Rho, implying that the hydrogen bond involving Glu122 in Meta-II_aH^+ is not altered in Meta-II_bH^+. For E134C, the double difference spectrum showed only the positive band at 1740 cm^{-1}, indicating the protonation of Glu134. Thus, the protonation site in Meta-II_aH^+ is Glu134, like that in Meta-II_bH^+. However, the frequency is significantly higher than that in Meta-II_bH^+ (1713 cm^{-1}) (16). Thus the hydrogen-bond involving Glu134 is weak in Meta-II_aH^+, and is strengthened in Meta-II_bH^+. Glu134 in Meta-II_bH^+ would be strongly hydrogen-bonded with a water molecule penetrating into the transmembrane region, as suggested by the crystal structures of Meta-II (8) and opsin (37, 38).

Meta-II_aH^+/Rho spectra (single diffrence spectra) of wild-type and the mutants in 1800-800 cm^{-1} region are shown in Figure 4. They all exhibited no marker band of Meta-I at 949 cm^{-1}, and weak intensity of the 1644 cm^{-1} band specific for Meta-II_bH^+, implying that the introduction of cysteine does not largely affect the formation of Meta-II_aH^+, although the different intensity of 1644 cm^{-1} band suggests that the equilibrium constant between Meta-I_aH^+ and Meta-II_bH^+ varied among the mutants. It should be noted that the conformational changes of A117C, T118C, and W126C were also comparable to those of wild-type, while they showed significantly blue-shifted absorption spectra

Mapping of Structural Changes upon Formation of Meta-II_aH^+ Probed by S-H Stretching Modes- Meta-II_aH^+/Rho spectra in the S-H stretching region are shown in Figure 5. Meta-II_aH^+/Rho spectra of wild-type (light cyan lines) are superimposed on those of mutants (red lines), and the double difference spectra between wild-type and mutant spectra are shown beneath (blue lines). Among the spectra of the 7 cysteine-replaced mutants (Figures 5a-5g), the Meta-II_aH^+/Rho spectra of C167S and C185S were different from that of wild-type, indicating environmental changes at positions 167 and 185. The double difference spectra between wild-type and C167S and between wild-type and C185S exhibited bilobic bands at 2556/2569 cm^{-1} and 2546/2561 cm^{-1}, respectively (Figures 5b and 5c), implying that the hydrogen bonds involving Cys167 and Cys185 are strengthened upon formation of Meta-II_aH^+. Although the conformation around Cys316 changes upon formation of Gt-activating state (Meta-II_bH^+) (39), the S-H stretching vibrations of Cys316 were not perturbed in Meta-II_aH^+.

It has been speculated that cleavage of the disulfide bond between Cys110 and Cys187 might

occur upon formation of Meta-II based on the finding that the Meta-II/Rho spectrum shows only positive bands in the S-H stretching region (21). However, our results clearly showed that the Meta-II_aH^+/Rho spectra of C110A/C187A were identical with that of wild-type (Figure 5g), indicating that the disulfide bond is not cleaved.

The Meta-II_aH^+/Rho spectra of the cysteine-introduced mutants are shown in Figures 5h-5v. While the native cysteine residues were not replaced in these mutants, the vibrational band of introduced cysteine was assessed by the double difference spectra between cysteine-introduced mutants and wild-type, in which the contribution of native cysteine residues should be canceled.

Ala117, Thr118, and Glu122 are located in the immediate vicinity of the chromophore, and the introduction of the cysteine residue in these positions causes the blue-shifted absorption spectra (Table 1). The double difference spectrum for Meta-II_aH^+ of A117C had a broad and weak positive band at 2573 cm^{-1} (Figure 5h). A small positive band at 2553 cm^{-1} and negative bands at 2565 and 2532 cm^{-1} were observed for T118C (Figure 5i). The double difference spectrum for E122C shows a negative band at 2574 cm^{-1} and two positive bands at 2580 and 2563 cm^{-1} (Figure 5j). The two positive bands are likely to be caused by the heterogeneity of the S-H group in the Meta-II_aH^+. The possible heterogeneity at position 122 is also indicated by the C=O stretching band of Glu122 having a spectral shoulder (arrow in Figure 2d).

I123C had a positive band at 2580 cm^{-1} in the double difference spectrum for Meta-II_aH^+/Rho spectrum (Figure 5k). The band at 2580 cm^{-1} suggests that this S-H group does not form a hydrogen bond in Meta-II_aH^+ (20). Since the side chain of Ile123 is located on the opposite side of Helix III from the chromophore, and surrounded by Helices II, III and IV, small movements of these helices would take place upon Meta-II_aH^+ formation to disrupt the hydrogen bond of Cys123.

L125C and L128C displayed bilobic bands, indicating the frequency shift of S-H stretching modes. However, A124C, W126C, and S127C displayed only weak positive bands. Because the absence of the complementary band implies an intensity change with little frequency change of the S-H stretching band, these results suggest that only minor changes occurred in these positions. No environmental change of S-H group was observed for V129C, V130C, L131C, A132C, I133C or E134C, although Glu134 is involved in the conserved ERY sequence. Because large helical movement is suppressed in this condition, the environment around Cys134 would not be altered.

The environmental changes of amino acid residues probed in this study are shown in Figure 6. The positions of cysteine residues which showed frequency shifts in Meta-II_aH^+/Rho spectra are indicated in red, those with only intensity change in pink, and those with no change in white. The amino acid residues within 4 Å of amino acid residues where introduced cysteine showed frequency shifts were listed using PyMOL software. The results demonstrated that Ala164, His211, and Phe261 were located within 4 Å of two or more positions. It is an advantage of cysteine scanning over conventional point mutation method that the key amino acid residue is identified without mutation of itself, because mutation of key residue may substantially alters the nature.

DISCUSSION

The structural changes of rhodopsin in the transmembrane region were detected here by use of the cysteine S-H group as an internal probe. All mutants prepared in this study formed pigments with 11-*cis*-retinal and were converted to Meta-II_aH^+, which exhibited chromophore vibrational bands as well as amide-I bands very similar to those of the wild-type. These results indicate that the cysteine residue acts as a highly sensitive probe for conformational changes of the protein, although the introduction of a cysteine residue into the transmembrane region hardly perturbs the native structure. In the present study, a photoproduct which has a deprotonated chromophore but undergoes small conformational change was trapped in hydrated film sample of PC liposome at pH 5.7. While the characteristics of the FTIR spectrum of this photoproduct regarding the amide-I, Glu83, and Glu122 bands agreed with those of Meta-II_a reported previously (18), Glu134 in this photoproduct is protonated, whereas it is not protonated in Meta-II_a (Figure 2). Thus, this photoproduct was identified as Meta-II_aH^+.

Although there is no direct evidence showing the interconversion between Meta-II_aH^+ and Meta-II_bH^+, Meta-II_aH^+ and Meta-II_bH^+ would be in pH-independent equilibrium, like Meta-II_a and Meta-II_b. Meta-II_aH^+ would be enriched by suppression of the helical rearrangements in the hydrated film containing less water than in solution. PC is also

likely to bias the equilibrium towards Meta-II_aH^+. However, because Meta-II_aH^+ was trapped in the artificial condition, we could not exclude the possibility that the structure of Meta-II_a which is transiently formed in the physiological condition may be different from that of Meta-II_aH^+ observed here.

It is reported that the deprotonated intermediate is produced by irradiation of rhodopsin crystal (40). Crystal structure of this intermediate (2I37) demonstrated that the Helix V is elongated but the overall helical arrangement is close to the dark state unlike the G-protein-interacting conformation (3DQB, 3PQR and 2X72). Because the small conformational change would be derived from the crystal packing, 2I37 would represent the structure of Meta-II_a.

We probed the environmental changes for Meta-II_aH^+ at 23 positions (8 native cysteine residues plus 15 introduced cysteine residues) by analyzing S-H vibrational mode. Mapping of the cysteine residues showing S-H vibrational changes demonstrated that they are localized proximal to Ala164, His211 and Phe261 (Figure 6).

His211, which stabilizes the active conformation (41), is hydrogen-bonded with Glu122. The amino acid residue corresponding to Glu122 of rhodopsin is Gln in cone pigments, and this is one of the reasons why the decay of Meta-II of cone pigments is significantly faster than that of rhodopsin (42, 43). The environmental changes around His211 strongly suggest that the hydrogen bond between Glu122 and His211 is perturbed in Meta-II_aH^+. Environmental changes were also observed around Phe261, which forms the hydrophobic interface between helices III and IV together with Gly121, Leu125, and Trp265. These residues are essential for the correct folding of the pigment (44-46). Notably, mutants of these residues such as F261V and G121L/F261V show significant constitutive activity (47), suggesting that the disruption of this packing may result in the active conformation. It should be noted that these interpretations are based on the notion that Meta-II_aH^+ is a direct precursor of Meta-II_bH^+.

On the other hand, the S-H group of Cys222 in Helix V forms a hydrogen bond with the backbone carbonyl oxygen of Ala132 in Helix III in the dark state (1U19), while this hydrogen bond is disrupted in G-protein-interacting conformations (3DQB, 3PQR and 2X72). The lack of change in the S-H vibration of Cys222 suggests that the arrangements of Helices III and V are not altered in Meta-II_aH^+. In addition, the lack of environmental change at position 134, which is involved in the conserved ERY sequence and proximate to the Arg135/Glu247 ionic lock, also supports the notion that the conformational change is not propagated to the cytoplasmic side in Meta-II_aH^+.

In conclusion, the present results showed that the Glu122/His211 hydrogen bond, which stabilizes the active conformation, and the Gly121/Leu125/Phe261/Trp265 hydrophobic packing between Helices III and VI, which maintains the correct folding and suppresses the constitutive activity, are likely to be perturbed prior to the helical rearrangement. Protonation of Glu134 facilitates the deprotonation of the chromophore Schiff base but does not necessarily induce the great helical movements. The changes in the intramolecular interaction near the chromophore would induce the significant rearrangement of the transmembrane helices, resulting in the active conformation.

REFERENCES

1. Palczewski, K., Kumasaka, T., Hori, T., Behnke, C. A., Motoshima, H., Fox, B. A., Le Trong, I., Teller, D. C., Okada, T., Stenkamp, R. E., Yamamoto, M., and Miyano, M. (2000) Crystal structure of rhodopsin: A G protein-coupled receptor. *Science* **289**, 739-745
2. Rasmussen, S. G. F., Choi, H. J., Rosenbaum, D. M., Kobilka, T. S., Thian, F. S., Edwards, P. C., Burghammer, M., Ratnala, V. R. P., Sanishvili, R., Fischetti, R. F., Schertler, G. F. X., Weis, W. I., and Kobilka, B. K. (2007) Crystal structure of the human β_2 adrenergic G-protein-coupled receptor. *Nature* **450**, 383-387
3. Cherezov, V., Rosenbaum, D. M., Hanson, M. A., Rasmussen, S. G., Thian, F. S., Kobilka, T. S., Choi, H. J., Kuhn, P., Weis, W. I., Kobilka, B. K., and Stevens, R. C. (2007) High-resolution crystal structure of an engineered human β_2-adrenergic G protein-coupled receptor. *Science* **318**, 1258-1265
4. Farrens, D. L., Altenbach, C., Yang, K., Hubbell, W. L., and Khorana, H. G. (1996) Requirement of rigid-body motion of transmembrane helices for light activation of rhodopsin. *Science* **274**, 768-770
5. Sheikh, S. P., Zvyaga, T. A., Lichtarge, O., Sakmar, T. P., and Bourne, H. R. (1996) Rhodopsin activation blocked by metal-ion-binding sites linking transmembrane helices C and F. *Nature* **383**, 347-350
6. Dunham, T. D., and Farrens, D. L. (1999) Conformational changes in rhodopsin. Movement of helix F detected by site-specific chemical labeling and fluorescence spectroscopy. *J. Biol. Chem.* **274**, 1683-1690
7. Deupi, X., and Standfuss, J. (2011) Structural insights into agonist-induced activation of G-protein-coupled receptors. *Curr. Opin. Struct. Biol.* **21**, 541-551
8. Choe, H. W., Kim, Y. J., Park, J. H., Morizumi, T., Pai, E. F., Krauss, N., Hofmann, K. P., Scheerer, P., and Ernst, O. P. (2011) Crystal structure of metarhodopsin II. *Nature* **471**, 651-655
9. Standfuss, J., Edwards, P. C., D'Antona, A., Fransen, M., Xie, G., Oprian, D. D., and Schertler, G. F. (2011) The structural basis of agonist-induced activation in constitutively active rhodopsin. *Nature* **471**, 656-660
10. Deupi, X., Edwards, P., Singhal, A., Nickle, B., Oprian, D., Schertler, G., and Standfuss, J. (2012) Stabilized G protein binding site in the structure of constitutively active metarhodopsin-II. *Proc. Natl. Acad. Sci. U. S. A.* **109**, 119-124
11. Matthews, R. G., Hubbard, R., Brown, P. K., and Wald, G. (1963) Tautomeric Forms of Metarhodopsin. *J. Gen. Physiol.* **47**, 215-240
12. Parkes, J. H., and Liebman, P. A. (1984) Temperature and pH dependence of the metarhodopsin I-metarhodopsin II kinetics and equilibria in bovine rod disk membrane suspensions. *Biochemistry* **23**, 5054-5061

13. Imai, H., Mizukami, T., Imamoto, Y., and Shichida, Y. (1994) Direct observation of the thermal equilibria among lumirhodopsin, metarhodopsin I, and metarhodopsin II in chicken rhodopsin. *Biochemistry* **33**, 14351-14358
14. Sato, K., Morizumi, T., Yamashita, T., and Shichida, Y. (2010) Direct observation of the pH-dependent equilibrium between metarhodopsins I and II and the pH-independent interaction of metarhodopsin II with transducin C-terminal peptide. *Biochemistry* **49**, 736-741
15. Knierim, B., Hofmann, K. P., Ernst, O. P., and Hubbell, W. L. (2007) Sequence of late molecular events in the activation of rhodopsin. *Proc. Natl. Acad. Sci. U. S. A.* **104**, 20290-20295
16. Vogel, R., Mahalingam, M., Ludeke, S., Huber, T., Siebert, F., and Sakmar, T. P. (2008) Functional role of the "ionic lock"--an interhelical hydrogen-bond network in family A heptahelical receptors. *J. Mol. Biol.* **380**, 648-655
17. Mahalingam, M., Martinez-Mayorga, K., Brown, M. F., and Vogel, R. (2008) Two protonation switches control rhodopsin activation in membranes. *Proc. Natl. Acad. Sci. U. S. A.* **105**, 17795-17800
18. Zaitseva, E., Brown, M. F., and Vogel, R. (2010) Sequential rearrangement of interhelical networks upon rhodopsin activation in membranes: the Meta II_a conformational substate. *J. Am. Chem. Soc.* **132**, 4815-4821
19. Vogel, R., and Siebert, F. (2003) Fourier transform IR spectroscopy study for new insights into molecular properties and activation mechanisms of visual pigment rhodopsin. *Biopolymers* **72**, 133-148
20. Li, H., and Thomas, G. J., Jr. (1991) Cysteine conformation and sulfhydryl interactions in proteins and viruses. 1. Correlation of the Raman S-H band with hydrogen bonding and intramolecular geometry in model compounds. *J. Am. Chem. Soc.* **113** 456-462
21. Rath, P., Bovee-Geurts, P. H., DeGrip, W. J., and Rothschild, K. J. (1994) Photoactivation of rhodopsin involves alterations in cysteine side chains: detection of an S-H band in the Meta I→Meta II FTIR difference spectrum. *Biophys. J.* **66**, 2085-2091
22. Kandori, H., Kinoshita, N., Shichida, Y., Maeda, A., Needleman, R., and Lanyi, J. K. (1998) Cysteine S−H as a hydrogen-bonding probe in proteins. *J. Am. Chem. Soc.* **120**, 5828-5829
23. Yamazaki, Y., Nagata, T., Terakita, A., Kandori, H., Shichida, Y., and Imamoto, Y. (2014) Mapping of the local environmental changes in proteins by cysteine scanning. *Biophysics* **10**, 1-7
24. Ye, S., Zaitseva, E., Caltabiano, G., Schertler, G. F., Sakmar, T. P., Deupi, X., and Vogel, R. (2010) Tracking G-protein-coupled receptor activation using genetically encoded infrared probes. *Nature* **464**, 1386-1389
25. Nathans, J. (1990) Determinants of visual pigment absorbance: identification of the retinylidene Schiff's base counterion in bovine rhodopsin. *Biochemistry* **29**, 9746-9752
26. Fahmy, K., and Sakmar, T. P. (1993) Regulation of the rhodopsin-transducin interaction by a

highly conserved carboxylic acid group. *Biochemistry* **32**, 7229-7236

27. Okada, T., Ernst, O. P., Palczewski, K., and Hofmann, K. P. (2001) Activation of rhodopsin: new insights from structural and biochemical studies. *Trends Biochem. Sci.* **26**, 318-324
28. Zhukovsky, E. A., and Oprian, D. D. (1989) Effect of carboxylic acid side chains on the absorption maximum of visual pigments. *Science* **246**, 928-930
29. Imai, H., Kefalov, V., Sakurai, K., Chisaka, O., Ueda, Y., Onishi, A., Morizumi, T., Fu, Y., Ichikawa, K., Nakatani, K., Honda, Y., Chen, J., Yau, K. W., and Shichida, Y. (2007) Molecular properties of rhodopsin and rod function. *J. Biol. Chem.* **282**, 6677-6684
30. Nathans, J., Weitz, C. J., Agarwal, N., Nir, I., and Papermaster, D. S. (1989) Production of bovine rhodopsin by mammalian cell lines expressing cloned cDNA: spectrophotometry and subcellular localization. *Vision Res.* **29**, 907-914
31. Nagata, T., Terakita, A., Kandori, H., Shichida, Y., and Maeda, A. (1998) The hydrogen-bonding network of water molecules and the peptide backbone in the region connecting Asp83, Gly120, and Glu113 in bovine rhodopsin. *Biochemistry* **37**, 17216-17222
32. Arnis, S., and Hofmann, K. P. (1993) Two different forms of metarhodopsin II: Schiff base deprotonation precedes proton uptake and signaling state. *Proc. Natl. Acad. Sci. U. S. A.* **90**, 7849-7853
33. Ohkita, Y. J., Sasaki, J., Maeda, A., Yoshizawa, T., Groesbeek, M., Verdegem, P., and Lugtenburg, J. (1995) Changes in structure of the chromophore in the photochemical process of bovine rhodopsin as revealed by FTIR spectroscopy for hydrogen out-of-plane vibrations. *Biophys. Chem.* **56**, 71-78
34. Nishimura, S., Sasaki, J., Kandori, H., Lugtenburg, J., and Maeda, A. (1995) Structural changes in the lumirhodopsin-to-metarhodopsin I conversion of air-dried bovine rhodopsin. *Biochemistry* **34**, 16758-16763
35. Jäger, F., Fahmy, K., Sakmar, T. P., and Siebert, F. (1994) Identification of glutamic acid 113 as the Schiff base proton acceptor in the metarhodopsin II photointermediate of rhodopsin. *Biochemistry* **33**, 10878-10882
36. Fahmy, K., Jäger, F., Beck, M., Zvyaga, T. A., Sakmar, T. P., and Siebert, F. (1993) Protonation states of membrane-embedded carboxylic acid groups in rhodopsin and metarhodopsin II: a Fourier-transform infrared spectroscopy study of site-directed mutants. *Proc. Natl. Acad. Sci. U. S. A.* **90**, 10206-10210
37. Scheerer, P., Park, J. H., Hildebrand, P. W., Kim, Y. J., Krauss, N., Choe, H. W., Hofmann, K. P., and Ernst, O. P. (2008) Crystal structure of opsin in its G-protein-interacting conformation. *Nature* **455**, 497-502
38. Park, J. H., Scheerer, P., Hofmann, K. P., Choe, H. W., and Ernst, O. P. (2008) Crystal structure of the ligand-free G-protein-coupled receptor opsin. *Nature* **454**, 183-187

39. Imamoto, Y., Kataoka, M., Tokunaga, F., and Palczewski, K. (2000) Light-induced conformational changes of rhodopsin probed by fluorescent Alexa594 immobilized on the cytoplasmic surface. *Biochemistry* **39**, 15225-15233
40. Salom, D., Lodowski, D. T., Stenkamp, R. E., Le Trong, I., Golczak, M., Jastrzebska, B., Harris, T., Ballesteros, J. A., and Palczewski, K. (2006) Crystal structure of a photoactivated deprotonated intermediate of rhodopsin. *Proc. Natl. Acad. Sci. U. S. A.* **103**, 16123-16128
41. Weitz, C. J., and Nathans, J. (1992) Histidine residues regulate the transition of photoexcited rhodopsin to its active conformation, metarhodopsin II. *Neuron* **8**, 465-472
42. Imai, H., Kojima, D., Oura, T., Tachibanaki, S., Terakita, A., and Shichida, Y. (1997) Single amino acid residue as a functional determinant of rod and cone visual pigments. *Proc. Natl. Acad. Sci. U. S. A.* **94**, 2322-2326
43. Imamoto, Y., Seki, I., Yamashita, T., and Shichida, Y. (2013) Efficiencies of activation of transducin by cone and rod visual pigments. *Biochemistry* **52**, 3010−3018
44. Nakayama, T. A., and Khorana, H. G. (1991) Mapping of the amino acids in membrane-embedded helices that interact with the retinal chromophore in bovine rhodopsin. *J. Biol. Chem.* **266**, 4269-4275
45. Han, M., Lin, S. W., Smith, S. O., and Sakmar, T. P. (1996) The effects of amino acid replacements of glycine 121 on transmembrane helix 3 of rhodopsin. *J. Biol. Chem.* **271**, 32330-32336
46. Hwa, J., Garriga, P., Liu, X., and Khorana, H. G. (1997) Structure and function in rhodopsin: packing of the helices in the transmembrane domain and folding to a tertiary structure in the intradiscal domain are coupled. *Proc. Natl. Acad. Sci. U. S. A.* **94**, 10571-10576
47. Han, M., Lin, S. W., Minkova, M., Smith, S. O., and Sakmar, T. P. (1996) Functional interaction of transmembrane helices 3 and 6 in rhodopsin. Replacement of phenylalanine 261 by alanine causes reversion of phenotype of a glycine 121 replacement mutant. *J. Biol. Chem.* **271**, 32337-32342

Acknowledgements- We are grateful to Prof. Robert S. Molday of University of British Columbia for providing the hybridoma producing rho 1D4 antibody and Dr. Takahiro Yamashita of Kyoto University for providing the rhodopsin E134C mutant plasmid clone. We are also grateful to Dr. Elizabeth Nakajima for critical reading of our manuscript and invaluable comments.

FOOTNOTES

*This work was supported in part by Grants-in-Aid for Scientific Research to YY, AT, HK, YS and YI from the Japanese Ministry of Education, Culture, Sports, Science and Technology.

[1]To whom correspondence should be addressed: Yasushi Imamoto, Department of Biophysics, Graduate School of Science, Kyoto University, Kyoto 606-8502, Japan, Tel.: +81-75-753-4243; Fax: +81-75-753-4210; E-mail: imamoto@rh.biophys.kyoto-u.ac.jp.

[2]The abbreviations used are: GPCR, G-protein-coupled receptor; Meta-I, metarhodopsin I; Meta-II, metarhodopsin II; FTIR, Fourier transform infrared; HOOP, hydrogen out-of-plane; DM, dodecyl-β-D-maltoside; PC, L-α-phosphatidylcholine; DOPC, 1,2-dioleoyl-*sn*-glycero-3-phosphocholine; ROS, rod outer segment.

FIGURE LEGENDS

Figure 1: **Secondary structural model of bovine rhodopsin.** Among the 10 native cysteine residues, 6 cysteine residues, which have free S-H groups (red), were replaced by serine residues (C140S, C167S, C185S, C222S, C264S, and C316S). Cys110 and Cys187, which form a disulfide bond (blue), were replaced by alanine residues (C110A/C187A). Alternatively, a cysteine residue was introduced into Helix III (A117C, T118C, E122C, I123C, A124C, L125C, W126C, S127C, L128C, V129C, V130C, L131C, A132C, I133C, and E134C) (green).

Figure 2: **FTIR spectra of metarhodopsins.** Meta-II_aH^+/Rho spectrum obtained by irradiation at 280 K (b) is compared with Meta-I/Rho (a) and Meta-II_bH^+/Rho (c) spectra. Meta-I/Rho and Meta-II_bH^+/Rho spectra were recorded using bovine ROS by irradiation at 240 K and 290 K, respectively. Meta-II_aH^+/Rho spectra of E122C (d) and E134C (e) are superimposed on that of wild-type (light cyan lines). The double difference spectra (wild-type spectra minus mutant spectra) are shown beneath (blue lines).

Figure 3: **The difference FTIR spectra before and after irradiation at 283 K.** curve 1: recombinant wild-type rhodopsin in PC liposome hydrated with 1 µL water (Meta-II_aH^+/Rho spectrum). curve 2: Linear combination of 0.78 Meta-I/Rho and 0.22 Meta-II_bH+/Rho spectra. curve 3: ROS hydrated with 1 µL water. curve 4: ROS hydrated with 1 µL of 60% glycerol/40% water. curve 5: ROS hydrated with 1 µL of 80% glycerol/20% water.

Figure 4: **Meta-II_aH^+/Rho spectra of wild-type and mutants in 1800-800 cm^{-1} region.** They were obtained by irradiation with >520-nm light at 280 K. The absorption maxima in the visible region are shown in the parentheses. The vibrational bands shifted from those of wild-type were indicated by triangles.

Figure 5: **Meta-II_aH^+/Rho spectra in the S-H stretching region.** Meta-II_aH^+/Rho spectra for mutants (red lines) are superimposed on that of wild-type (cyan lines). The double difference spectra are shown beneath (blue lines). Scale bar represents 1 x 10^{-4}. *Left.* Meta-II_aH^+/Rho spectra for the cysteine-substituted mutants (a-g). Double difference spectra were calculated by subtracting mutant spectra from wild-type spectra. *Middle and right.* Meta-II_aH^+/Rho spectra for cysteine-introduced mutants (h-v). Double difference spectra were calculated by subtracting wild-type spectra from mutant spectra. Typical frequency of S-H stretching mode is shown by the thick bar at the bottom of each panel.

Figure 6: **Mapping of cysteine residues that showed environmental changes.** The positions of cysteine residues that showed a frequency shift in Meta-II_aH^+/Rho spectra are indicated in red, those with only

intensity change in pink, and those with no change in white. The amino acid side chains are shown by spheres positioned at the β-carbons of the original amino acid residues. The crystal structure of lumirhodopsin (2HPY) was used as a template.

Table 1: Absorption maxima and optical purity indexes of recombinant rhodopsin mutants

mutant	λ_{max} (nm)[a]	optical purity[c]	mutant	λ_{max} (nm)	optical purity
Wild-type	499	1.8	A124C	499 (0)	2.2
C140S	499 (0)[b]	2.9	L125C	501 (+2)	1.8
C167S	497 (-2)	3.3	W126C	484 (-15)	2.8
C185S	501 (+2)	2.5	S127C	497 (-2)	2.0
C222S	500 (+1)	1.8	L128C	500 (+1)	1.9
C264S	501 (+2)	2.0	V129C	500 (+1)	2.2
C316S	500 (+1)	2.0	V130C	501 (+2)	2.0
C110A/C187A	497 (-2)	3.7	L131C	500 (+1)	2.1
A117C	488 (-11)	ND[d]	A132C	498 (-1)	2.1
T118C	484 (-15)	ND	I133C	498 (-1)	2.0
E122C	496 (-3)	2.1	E134C	500 (+1)	2.3
I123C	500 (+1)	1.9			

[a]Absorption maximum in the visible region. [b]Difference from wild-type is shown in parentheses. [c]Ratio of absorbance at 280 nm to absorbance at λ_{max}. [d]Not determined.

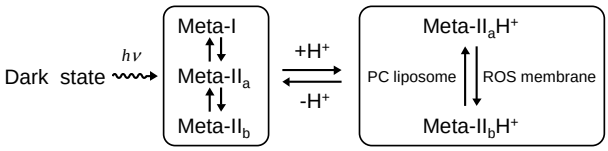

Scheme 1: Yamazaki et al.

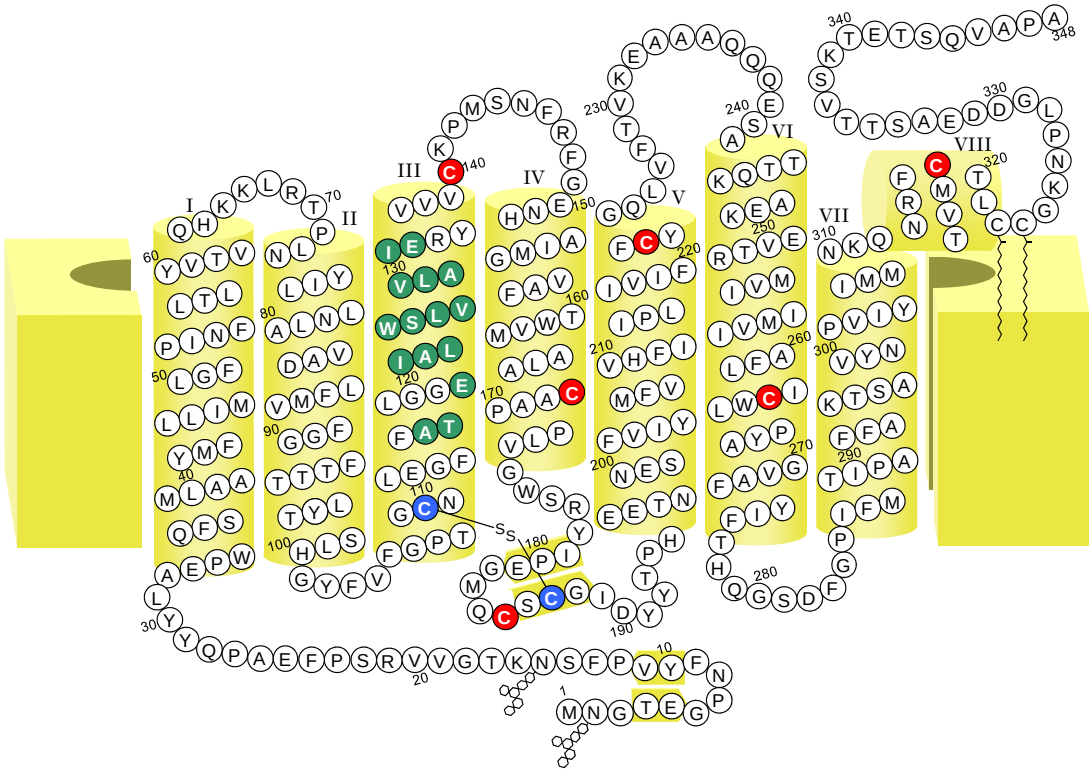

Figure 1: Yamazaki et. al.

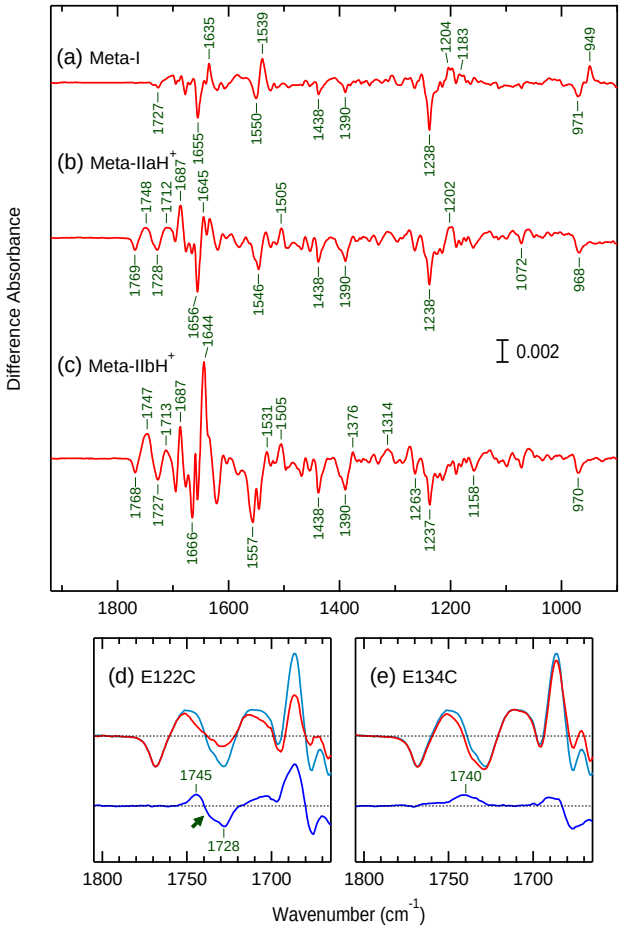

Figure 2: Yamazaki et. al.

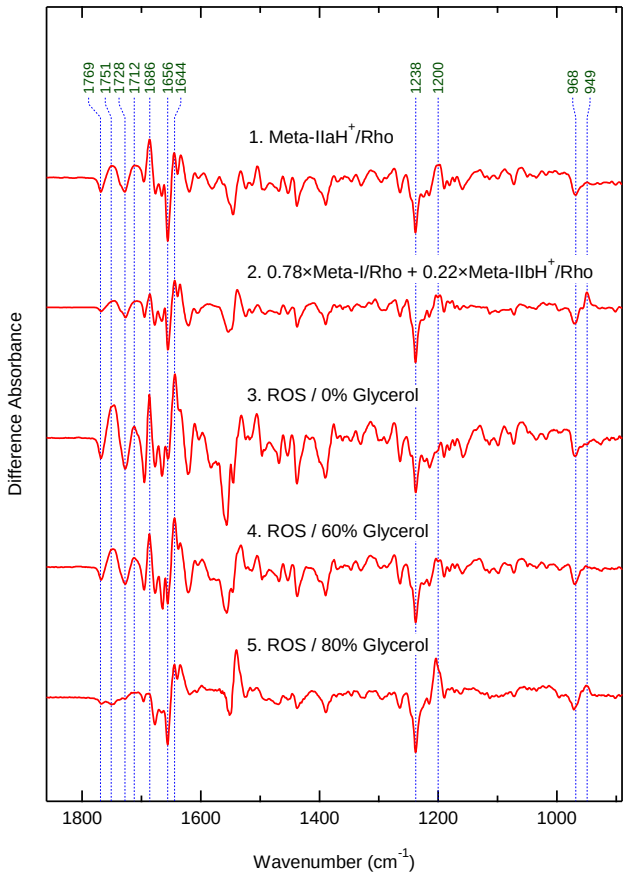

Figure 3: Yamazaki et. al.

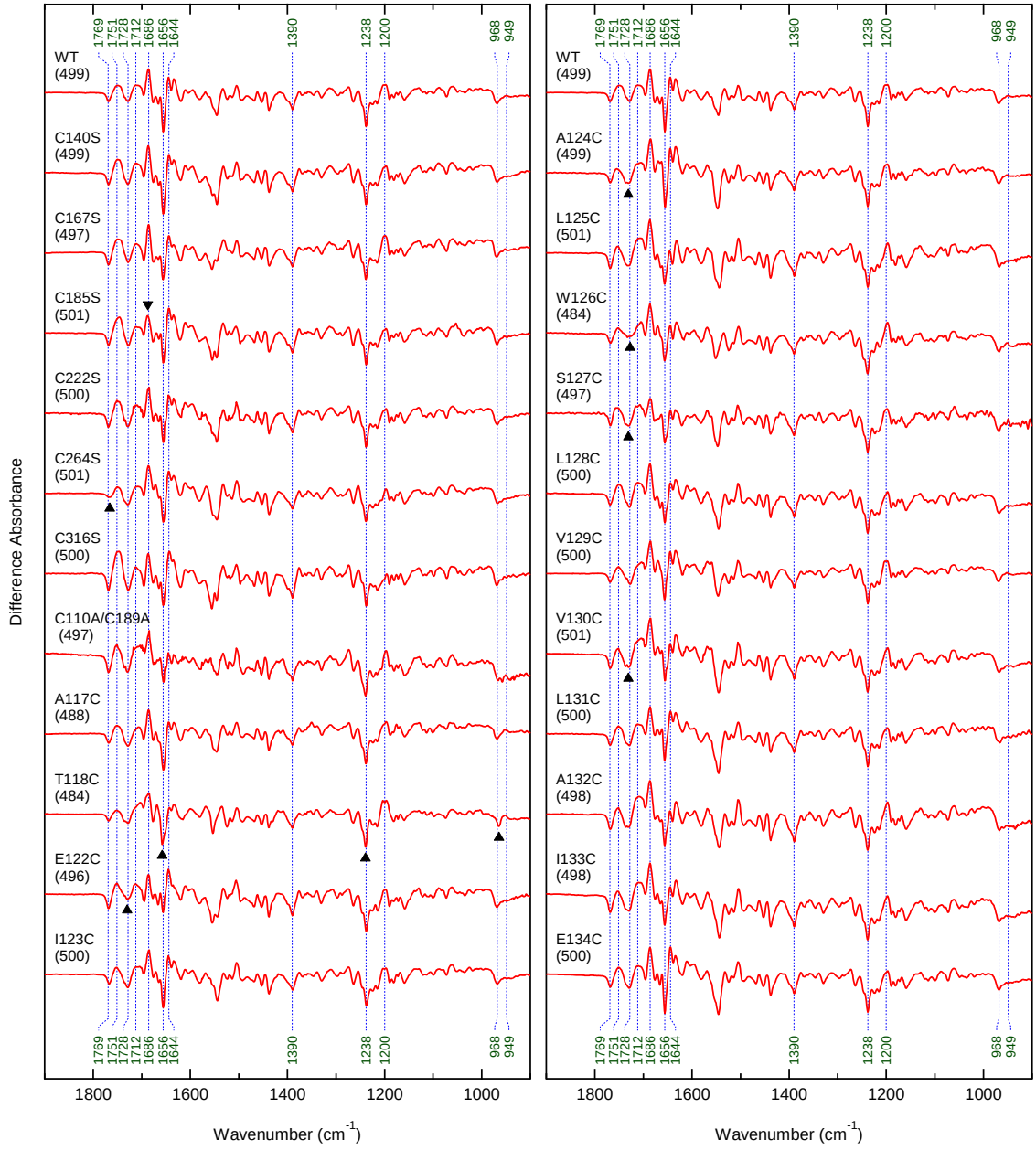

Figure 4: Yamazaki et. al.

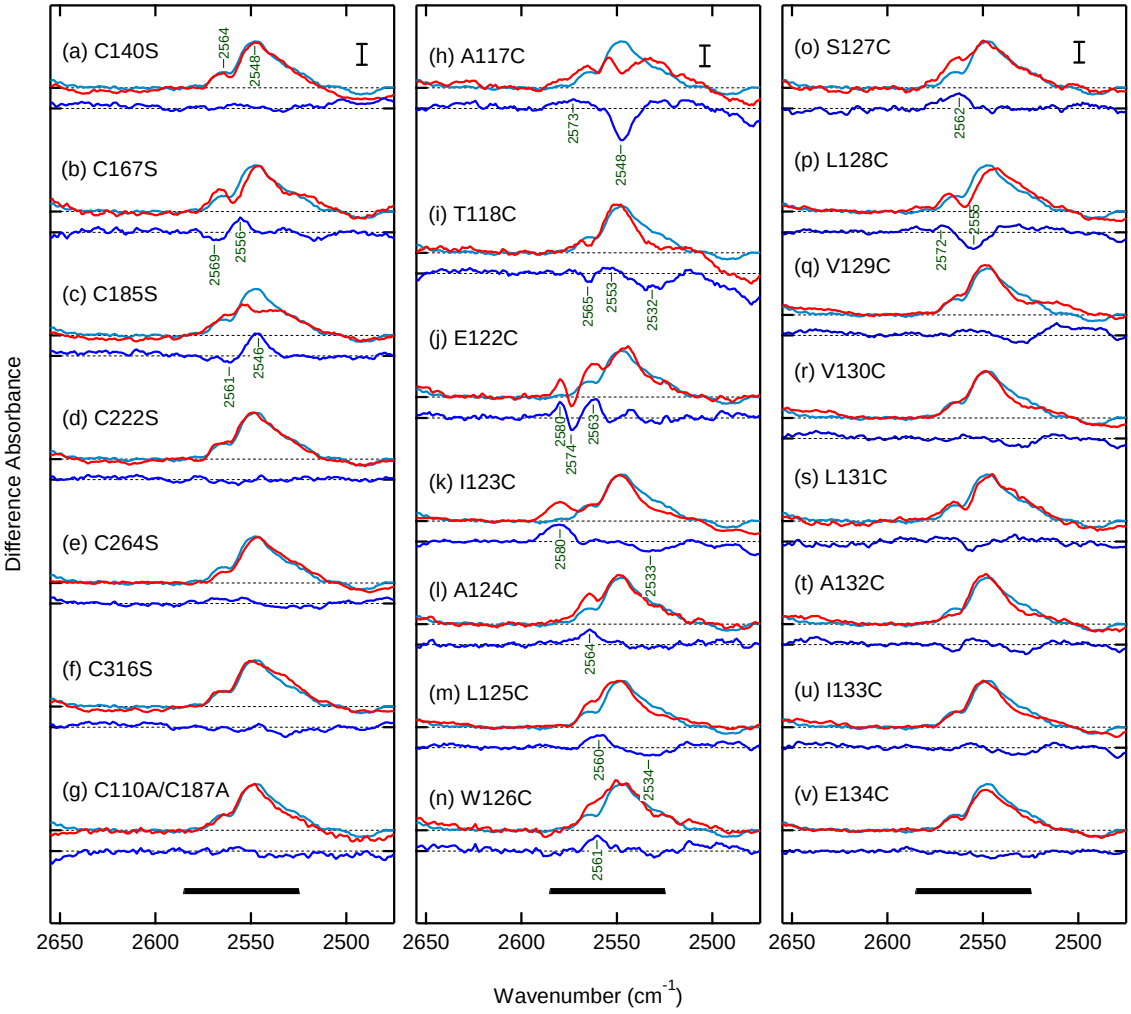

Figure 5: Yamazaki et. al.

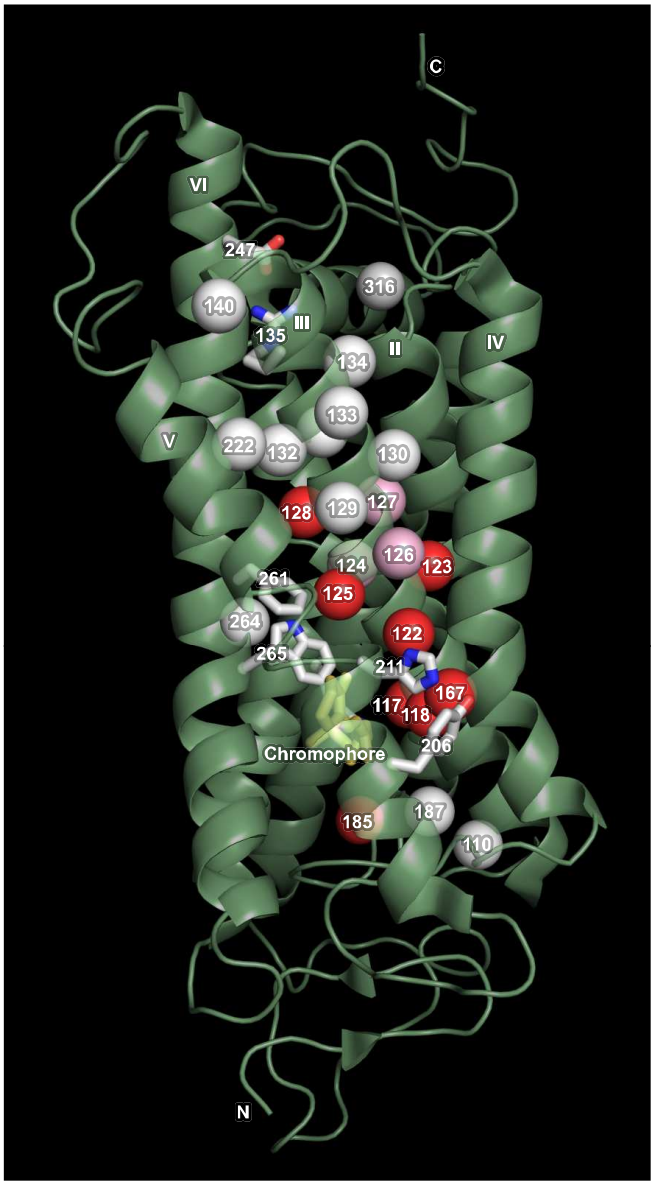

Figure 6: Yamazaki et. al.